J Solid State Electrochem (2005) 9: 524–530
DOI 10.1007/s10008-004-0607-9

ORIGINAL PAPER

G. G. Wang · J. M. Wang · W. Q. Mao · H. B. Shao
J. Q. Zhang · C. N. Cao

Physical properties and electrochemical performance of $LiMn_2O_4$ cathode materials prepared by a precipitation method

Received: 3 August 2004 / Revised: 9 August 2004 / Accepted: 10 October 2004 / Published online: 16 December 2004

Abstract $LiMn_2O_4$ powder for lithium-ion batteries was prepared by a precipitation method, and the effects of calcination temperature on the physical properties and electrochemical performance of the samples were investigated by various methods. The results of X-ray diffraction (XRD) showed that the lattice parameter (*a*) and the unit cell volume (*v*) decrease with the increasing calcination temperature, and the $LiMn_2O_4$ sample calcined at 750°C has smaller particle size and higher crystallinity than other samples. The results of the electrochemical experiments showed that the sample calcined at 750°C has larger peak currents, higher initial capacity, and better cycling capability, because of its lower charge-transfer resistance and larger diffusion coefficient of Li^+ ions than those of other samples.

Keywords $LiMn_2O_4$ · Precipitation method · Cyclic voltammetry · Electrochemical impedance spectroscopy

Introduction

Lithium-ion batteries have recently been widely applied in high-tech electronics such as mobile telephones and notebook computers, owing to their high working voltage, large specific energy, low self-discharge rate, and elevated energy density [1–3]. In these batteries, lithiated transition metal oxides such as $LiCoO_2$, $LiNiO_2$ or $LiMn_2O_4$ are used as cathode materials, with carbon as the anode material. Among these cathode materials, $LiMn_2O_4$ has been intensively developed because it is inexpensive, has acceptable environmental characteristics, and is safer than $LiCoO_2$ [4, 5]. In recent years, much effort has been devoted to the synthesis of powders for enhancing their cycleability and specific capacity [6–8].

$LiMn_2O_4$ samples are usually prepared by a conventional solid-state reaction [9–12]. In this process, the oxides or carbonates containing manganese and lithium cations are physically mixed by mechanical methods, and all the solid particles might not completely react, which results in undesirable impurities in the final product. In recent years, several kinds of low temperature-preparation technique such as sol–gel precipitation [13], the Pechini process [14], and emulsion [15, 16] and electrochemical [17, 18] processes have been developed. All the components can be homogeneously distributed in samples prepared by these low-temperature techniques. Single-phase products with good crystallizability, homogeneity, and uniform particle morphology were obtained, which had high electrochemical activity. But the soft chemistry method and template method of synthesizing cathode materials are complicated and restricted, so it is valuable to explore simple and controllable methods of preparing $LiMn_2O_4$ samples with high activity and homogeneous particle morphology.

Huang and Bruce [19] prepared a precursor of $LiMn_2O_4$ from $Mn(CH_3COO)_2.4H_2O$ and Li_2CO_3 by a simple liquid-state precipitation method. The final $LiMn_2O_4$ sample with initial discharge capacity of 110 mAh g^{-1} and good capacity retention was obtained by calcining the precursor at 600°C. However, the effects of calcination temperature on the physicochemical properties of the samples have not been investigated.

In the work discussed in this paper, the method of synthesizing $LiMn_2O_4$ on the basis of Ref. [19] was improved, and the effects of calcination temperature on the physical properties and electrochemical performance of $LiMn_2O_4$ samples were investigated.

G. G. Wang · J. M. Wang (✉) · W. Q. Mao
H. B. Shao · J. Q. Zhang · C. N. Cao
Department of Chemistry, Zhejiang University,
Hangzhou, 310027, People's Republic of China
E-mail: wjm@cmsce.zju.edu.cn
Tel.: +86-571-87951513
Fax: +86-571-87953309

J. Q. Zhang · C. N. Cao
Chinese State Key Laboratory for Corrosion
and Protection, Shenyang, 110015,
People's Republic of China

Experimental

Preparation of samples

Li_2CO_3 and $Mn(CH_3COO)_2.4H_2O$ in 1:2 Li:Mn mole ratio were dissolved in distilled water. A precipitate (the precursor) was obtained by evaporating water with continual stirring at 95°C. The precursor was transferred into a ceramic crucible subsequently calcined in a Nabertherm furnace at temperatures ranging from 350 to 800°C for 8 h and then cooled slowly to room temperature in air. The heating and cooling rates were 3 and 1° min^{-1}, respectively.

Physical characterization of samples

Thermogravimetric analysis (TGA) and differential scanning calorimetry (DSC) were performed using a Netzsch STA409PC thermal analyzer and heating from room temperature to 800°C at a rate of 10° min^{-1}. Fourier transform infrared (FT-IR) spectroscopy of the samples was performed using a Nicolet Nexus 360 FT-IR spectrophotometer. A total of 1.5 mg sample dried at 120°C was thoroughly mixed with 200 mg KBr and pressed into pellets and the scans were performed immediately to avoid water absorption. The frequency range was 4000–350 cm^{-1}. The crystal structure of the samples was determined by X-ray diffraction (XRD) analysis using an X-ray diffractometer (Rigaku D/Max 2550) with Cu Kα radiation at 40 kV and 300 mA, and a scanning rate of 8° (2θ) per minute. The morphology of the samples was examined using scanning electron microscopy (SEM) (Sirion, Edax).

Preparation of electrodes and electrochemical tests

The charge and discharge characteristics of $LiMn_2O_4$ cathodes were examined in two-electrode test cells. The cells consisted of a cathode and a lithium metal anode separated by a microporous polypropylene separator. The electrolyte used was 1 mol L^{-1} $LiPF_6$ in a 50/50 vol.% mixture of ethylene carbonate (EC)/dimethyl carbonate (DMC). The cathode consisted of a mixture of 80 wt.% $LiMn_2O_4$, 10 wt.% acetylene black, and 10 wt.% polyvinylidene fluoride (PVDF). The mixture was pressed on to aluminium foil at 250 kg cm^{-2} and vacuum-dried at 120°C for 12 h. The cathode was cycled in the potential range 3.0–4.3 V versus Li/Li^+ at room temperature at different rates. Cyclic voltammetry (CV) was carried out in Swagelock three-electrode test cells [20] using Li foil as the counter electrode and reference electrode, at a scan rate of 0.05 mV s^{-1} between 3.0 and 4.3 V versus Li/Li^+. Electrochemical impedance spectroscopy (EIS) measurements were performed using a Swagelock three-electrode cell by means of a Potentiostat/Galvanostat Model 273A in conjunction with a model 5210 lock-in amplifier. A typical cathode was prepared by mixing 80 wt.% $LiMn_2O_4$, 10 wt.% acetylene black, and 10 wt.% PVDF and roll-pressed into a thin disk approximately 110 μm in thickness and 2.40 cm in diameter. The counter electrode and reference electrodes were made of Li foil. In EIS measurement the range of frequency was between 0.005 Hz and 120 kHz and the excitation amplitude was 5 mV. All assemble of the cell was carried out in a glove box filled with Ar gas.

Results and discussion

Physical properties of samples

Figure 1 shows the TGA–DSC curves of the precursor. There are two weight-loss regions on the curves. The first region, from room temperature to 200°C, might be attributed to the removal of bonded and absorbed water. During the second region of weight loss, from 240 to 350°C, one sharp exothermic reaction peak at 320°C is considered to be due to the decomposition of acetate and carbonate, for which weight loss is noticeable, and then the $LiMn_2O_4$ phase is formed. In the region from 350 to 800°C, the TGA curve becomes flat and no sharp peaks can be observed in the DSC curve, indicating that no phase transformation occurs.

Vibrational modes attributed to the motion of cations with respect to their oxygen neighbors are sensitive to the point group symmetry of the cations in the oxygen host matrix [21]. Hence, the local environment of the cations in a lattice of close-packed oxygen can be studied by FT-IR spectroscopy [22]. Infrared spectra of $LiMn_2O_4$ samples synthesized at different temperatures are shown in Fig. 2. The observed high-frequency bands, located around 618 and 517 cm^{-1}, are associated with the asymmetric stretching modes of MnO_6 group. These results are quite similar to those given in earlier reports [23, 24]. It can also be seen from Fig. 2 that the vibration

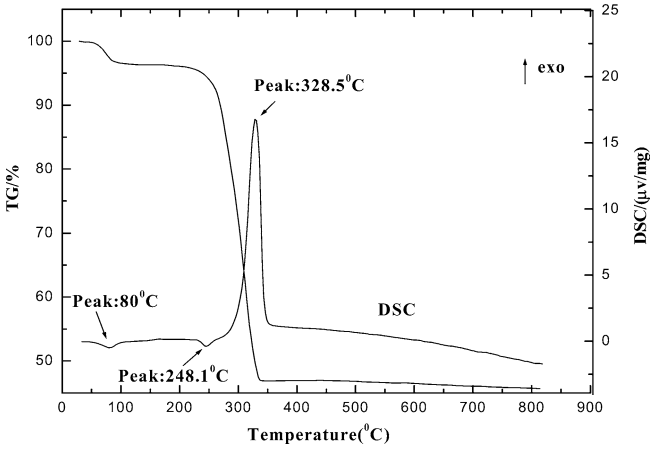

Fig. 1 TG–DSC curves of the $LiMn_2O_4$ sample

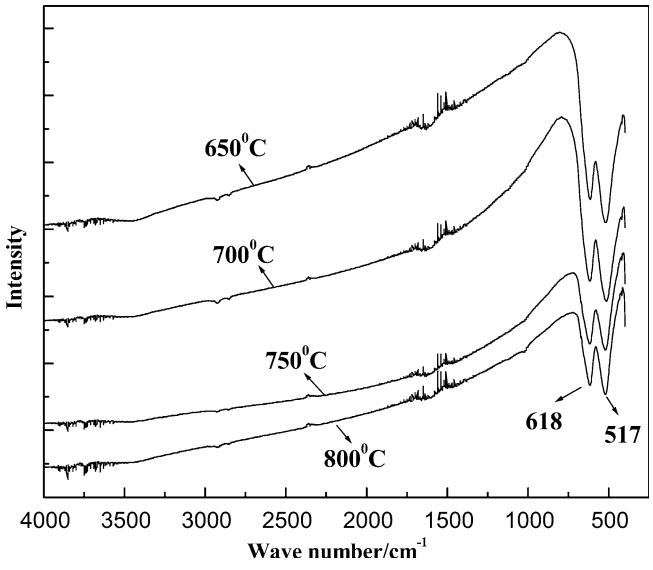

Fig. 2 FT-IR spectra of $LiMn_2O_4$ samples calcined at different temperatures

frequency of two stretching modes in the MnO_6 group do not change with increasing calcination temperature.

Figure 3 shows the XRD patterns of $LiMn_2O_4$ samples calcined at different temperatures in air. The XRD patterns of all the samples show the characteristics of the spinel $LiMn_2O_4$ structure (JCPDS 35-782) with space group Fd3m, which indicates the formation of the spinel $LiMn_2O_4$ structure at 350°C. The diffraction peaks of the sample calcined at 350°C are broad and weak. The existence of MnO and Mn_3O_4 impurity phases in the sample calcined at 350°C indicates that decomposition of acetate and carbonate occurs. As the calcination temperature increases, the diffraction peaks become sharper, the impurity phases of MnO and Mn_3O_4 disappear, and another impurity phase, Mn_2O_3, occurs. Even though the time of calcination at 700°C was prolonged to 16 h, the Mn_2O_3 impurity phase was still present in the $LiMn_2O_4$ sample. When the calcination temperature is increased to 750°C, the Mn_2O_3 impurity phase disappears and the pure spinel $LiMn_2O_4$ structure forms, which indicates that pure spinel $LiMn_2O_4$ can be produced by heat treatment at relatively high temperatures. This is obviously different from the results of Huang et al. [19], but is in agreement with the results from TGA-DSC analyses. Considering the sensitivity of the (311) and (400) peaks to annealing temperature and the intensity and positions of the peaks in the (311) and (400) diffraction lines [25, 26], those two peaks were chosen for estimation of the crystallinity of the samples. Table 1 shows the unit cell data for samples calcined at different temperatures. It can be seen that the lattice parameter (a) and the unit cell volume (v) decrease with increasing calcination temperature; this might have resulted from volatilization of small amount of lithium from the samples [1]. It also means that $LiMn_2O_4$ samples calcined at relatively high temperature might have better electrochemical performance [15, 27]. The FWHM values of the (311) and (400) diffraction lines of $LiMn_2O_4$ samples decrease with increasing calcination temperature and then increase; the minimum values are reached at 750°C. This indicates that the $LiMn_2O_4$ sample calcined at 750°C might have higher crystallinity, better ordering of local structure, and lower lattice strain.

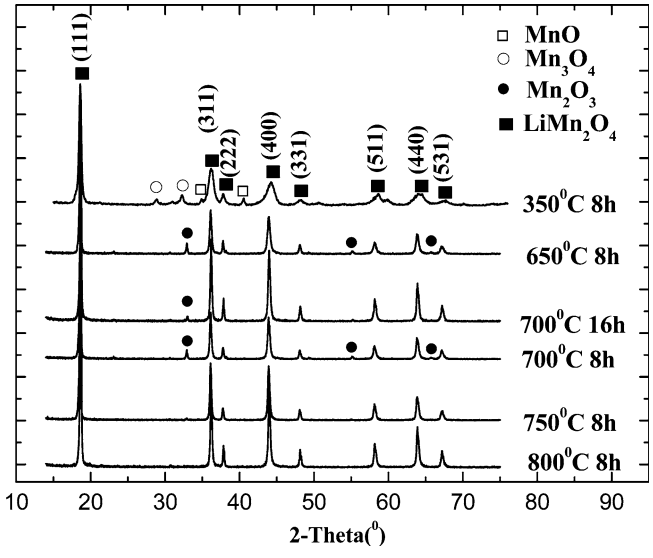

Fig. 3 X-Ray Diffraction patterns of samples calcined at different temperatures

Figure 4 shows scanning electron micrographs (SEM) obtained from $LiMn_2O_4$ samples calcined at different temperatures. The sample calcined at 750°C appears to be uniform irregular particles with some agglomeration; the average particle size is about 0.3 μm. The samples calcined at 700 and 800°C seem to be aggregates of irregular shape and their particle sizes are much larger than that of the sample calcined at 750°C. This indicates that the sample calcined at 750°C might have relatively higher rate capability. The greater extent of agglomeration of particles in the sample calcined at 800°C might have resulted from the higher calcination temperature; the serious agglomeration of particles in the sample calcined at 700°C might be related to the presence of Mn_2O_3 impurity phase.

Table 1 The cell parameters and cell volumes of samples calcined at different temperatures

	Sample (650°C)	Sample (700°C)	Sample (750°C)	Sample (800°C)
Lattice parameter a (Å)	8.24218	8.24131	8.24016	8.23376
Unit cell volume v (Å^3)	559.92	559.74	559.51	558.21
$FWHM_{(311)}$ (°)	0.267	0.239	0.204	0.211
$FWHM_{(400)}$ (°)	0.391	0.326	0.263	0.276

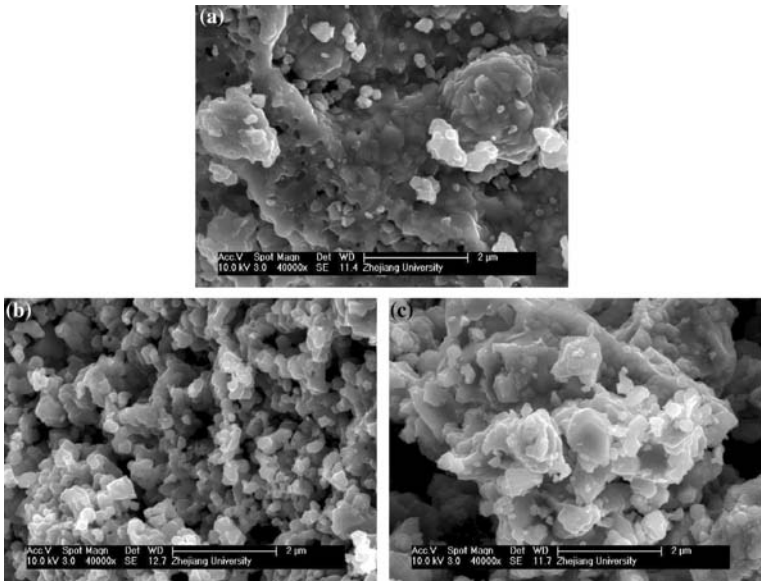

Fig. 4 Scanning electron microscopy photos of samples calcined at different temperatures **a** 700°C, **b** 750°C and **c** 800°C

Electrochemical performance of samples

Figure 5 shows cyclic voltammograms obtained, at a scanning rate of 0.05 mV s^{-1}, from samples calcined at different temperatures. It can be seen from Fig. 5 that there are two pairs of redox current peaks at about 3.92 V/4.10 V and 4.05 V/4.23 V on each cyclic voltammogram. These two pairs of redox peaks correspond to a two-step reversible intercalation reaction, in which lithium ions occupy two different tetragonal 8a sites in spinel $Li_xMn_2O_4$ ($x < 1$) [28]. It is apparent that the $LiMn_2O_4$sample calcined at 750°C has larger peak currents than other samples, which indicates that this sample might have greater electrochemical activity.

Figure 6 shows the first charge–discharge curves, at 0.2 and 0.5 C, of $LiMn_2O_4$ samples calcined at different temperatures. It can be seen that both the charge

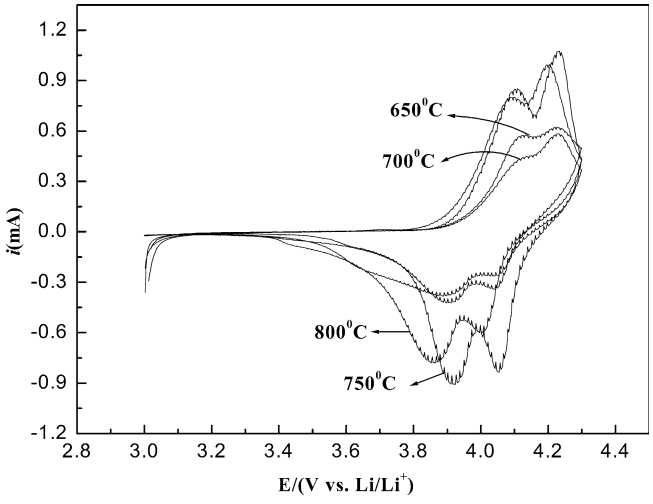

Fig. 5 Cyclic voltammograms obtained, at a scanning rate of 0.05 mV s^{-1}, from samples calcined at different temperatures

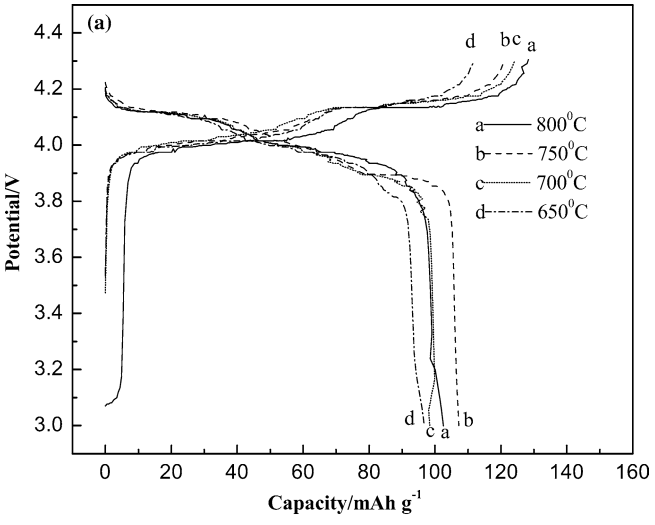

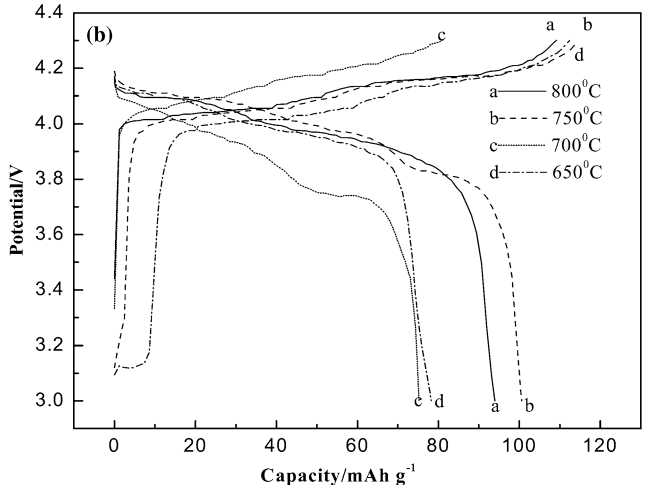

Fig. 6 The first charge–discharge curves of the samples calcined at different temperatures: **a** 0.2 C rate and **b** 0.5 C rate

and discharge curves have two distinct potential plateaus, which is in agreement with the results from the preceding cyclic voltammograms. The upper plateau region of the discharge curve represents a two-phase equilibrium between λ-MnO_2 and $Li_{0.5}Mn_2O_4$, whereas the second plateau represents a phase equilibrium between $Li_{0.5}Mn_2O_4$ and $LiMn_2O_4$ [29]. The discharge capacity first increases with increasing calcination temperature and then decreases. The largest discharge capacity occurs at 750°C, and the maximum values are 107 and 102 $mAhg^{-1}$ at 0.2 and 0.5 C, respectively. It can also be seen from Fig. 6 that the discharge capacity ratios (0.5 C/0.2 C) for samples calcined at 650, 700, 750, and 800°C is, respectively, 80.5, 76.3, 95.3, and 91.7%. These results show that the sample calcined at 750°C has not only higher discharge potential and larger discharge capacity but also better discharge capability at the relatively high rate, which is closely related to its structural characteristics, that is, smaller unit cell volume, higher crystallinity, and smaller particle size.

The electrochemical cyclic behavior of $Li/LiMn_2O_4$ cells at 0.2 and 0.5 C rates is presented in Fig. 7. The sample calcined at 650°C has a lower discharge capacity during all electrochemical cycles, which might be a result of the presence of impurity phase (Mn_2O_3). The sample calcined at 750°C has a larger discharge capacity and better electrochemical cycle stability, which can be attributed to its improved structure. The lower crystallinity of the sample calcined at 700°C might lead to its worse electrochemical cycle stability [30]. The large extent of agglomeration of particles might be the reason why the sample calcined at 800°C has lower electrochemical performance than that calcined at 750°C.

To investigate further the effects of calcination temperature on the kinetics of the electrode processes, the EIS of electrodes prepared using $LiMn_2O_4$ samples calcined at various temperatures were measured at open-circuit potentials. The EIS patterns displayed at Fig. 8 consist of two semicircles and a straight line. The small semicircle appearing in the high-frequency region reflects the resistance (R_f) of migration of Li^+ ions through the surface films, and film capacitance (C_f) [31–33]. The middle-frequency capacitive loop is caused by charge transfer resistance (R_t) and interfacial capacitance (C_{dl}). The low-frequency straight line can be attributed to diffusion of Li^+ ions in the samples. The characteristics of these electrodes, represented by the equivalent circuit, are shown in Fig. 9, where R_S is the total ohmic resistance of the electrode system, R_f and C_f are, respectively, the resistance and capacitance of a solid electrolyte interphase (SEI) film, and W is the Warburg impedance of solid-phase diffusion.

Fitted results from EIS are displayed in Table 2. It can be seen from Table 2 that the R_f values of different samples are almost constant, whereas R_t, W, and C_{dl}

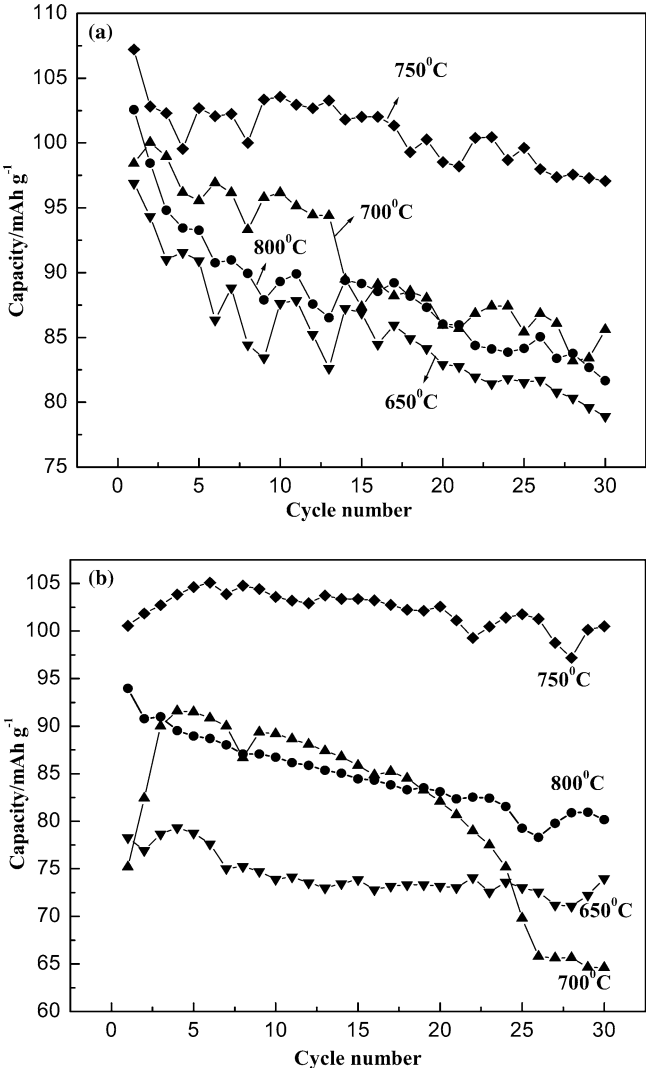

Fig. 7 The cycle performance of the samples calcined at different temperatures **a** 0.2 C and **b** 0.5 C

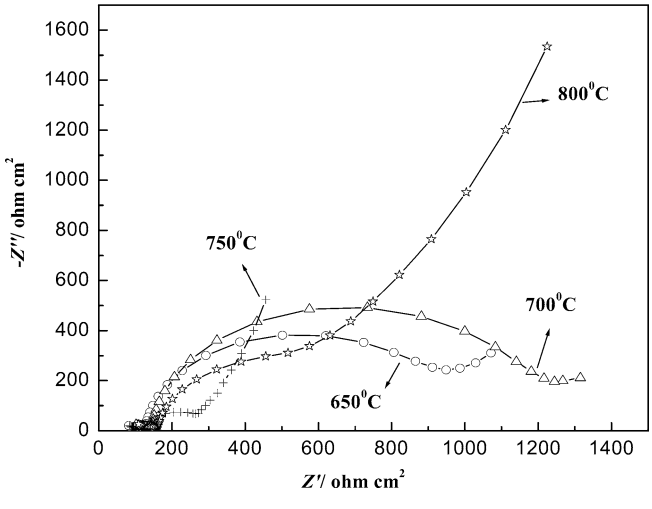

Fig. 8 Nyquist plots obtained, at open-circuit potentials, from electrodes prepared using $LiMn_2O_4$ samples calcined at different temperatures

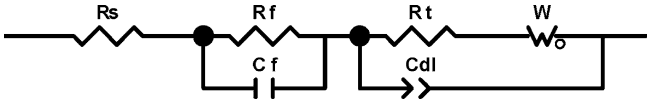

Fig. 9 Equivalent circuit used to analyze the EIS

Table 2 Some data obtained by EIS fitting

	Sample (650°C)	Sample (700°C)	Sample (750°C)	Sample (800°C)
R_f (ohm cm^2)	37.05	35.83	35.92	41.80
R_t (ohm cm^2)	747.9	945.9	130.95	427.5
W (ohm cm^2)	497.7	451.35	74.7	203.85
C_{dl} (mF cm^{-2})	5.07	2.07	7.64	10.22

values vary greatly with changing calcination temperature. The minimum R_t and W values of the sample calcined at 750°C mean the lowest electrochemical and diffusion polarization, and this leads to higher discharge potential at high rate. The larger R_t and W values indicate that the two samples calcined at 650 and 700°C have larger electrochemical and diffusion polarization, which results in their relatively lower discharge potential. Larger diffusion polarization resulting from low crystallinity and larger particle size is the main reason why the sample calcined at 700°C has worse activation performance and much lower discharge potential in the initial stage of the electrochemical cycle at a high rate.

It is instructive to compare the values of the interfacial capacitance (C_{dl}) from the middle-frequency semicircle [34]. It should also be noted from Table 2 that the interfacial capacitance (C_{dl}) has rather high values (2–11 mF cm^{-2}), which means that the electrode has a very large surface area. This might have resulted from the porous structure of the electrode and the rough surface of $LiMn_2O_4$ samples [35]. This result is in agreement with that of SEM.

Conclusions

1. $LiMn_2O_4$ cathode material has been prepared by a precipitation method using Li_2CO_3 and $Mn(CH_3COO)_2.4H_2O$. Weight loss of the precursor occurs and formation of the spinel $LiMn_2O_4$ phase starts below 350°C. Results from SEM and XRD showed that the cell parameter and the unit cell volume decrease with increasing calcination temperature, and the $LiMn_2O_4$ sample formed at 750°C has a smaller particle size and higher crystallinity than other samples.
2. The discharge potential and discharge capacity of the $LiMn_2O_4$ samples first increase and then decrease with increasing calcination temperature. The sample calcined at 750°C has a higher discharge potential, a larger discharge capacity, and better electrochemical cyclic stability than the other samples, because of the lower electrochemical and diffusion polarization which result from its smaller unit cell volume, higher crystallinity, and smaller particle size. Samples calcined at lower temperatures ($\leq$ 700°C) have lower discharge potential and smaller discharge capacity because of the presence of impurity phases, low crystallinity, or poor microstructure.

Acknowledgements The authors gratefully acknowledge financial support from the Chinese State Key Laboratory for Corrosion and Protection.

References

1. Lu CH, Lin SW (2001) J Power Sources 97–98:458
2. Sun Yk (1997) Solid State Ionics 100:115
3. Amine K, Tukamoto H, Yasuka H, Fujila Y (1996) J Electrochem Soc 143:1607
4. Tarascon JM, Wang E, Shokoohi FK, Mc Kinnon WR, Colson S (1991) J Electrochem Soc 138:2859
5. Masquelier C, Tabuchi M, Ado K, Kanno R, Kobayashi Y, Maki Y, Nakamura O, Goodenough JB (1996) J Solid State Chem 123:255
6. Ye SH, LV JY, Gao XP, Wu F, Song DY (2004) Electrochim Acta 49:1623
7. Nakayama M, Watanabe K, Ikuta W, Uchimoto Y, Wakihara M (2003) Solid State Ionics 164:35
8. Wu XM, Li XH, Xiao ZB, Liu JB, Yan WB, Ma MY (2004) Materials Chemistry and Physics 84:182
9. Hurimoto H, Suzuoka K, Murakami T, Xia Y, Nakamura H, Yoshi M (1995) J Electrochem Soc 142:2178
10. Gumow RJ, Kock A, Thackeray MM (1994) Solid State Ionics 69:59
11. Kang SH, Goodrnough LB (2000) J Electrochem Soc 147:3621
12. Xia Y, Yoshio M (1997) J Electrochem Soc 144:4186
13. Liu W, Farrington GC, Chaput F, Dunn B (1996) J Electrochem Soc 143:879
14. Liu W, Kowal K, Farrington GC, (1996) J Electrochem Soc 143:3590
15. Hwang KT, Um WS, Lee H S, Song JK, Chung KW (1998) J Power Sources 74:169
16. Lu CH, Lin SW (2001) J Power Sources 93:14
17. Hill LI, Portal R, Verbaere A, Guyomard D (2001) Electrochem Solid State Lett 4:A180
18. Hill LI, Portal R, Salle GL, Verbaere A, Guyomard D (2001) Electrochem Solid State Lett 4:D1
19. Huang HT and Peter G. Bruce (1994) J Electrochem Soc 141:L106
20. Yu P, Popov BN, Ritter JA, White RE (1999) J Electrochem Soc 146:8
21. Rougier CJ, Nazri GA, Julien C (1997) Mater Res Soc Symp Proc 453:647
22. Rouier A, Nazri G, Julien C (1997) Ionics 3:170
23. Richardson TJ, Ross PN (1996) Mater Res Bull 31:935
24. Chitra S, Kalyani P, Mohan T, Massot M, Ziolkiewicz S, Gangadharan R, Eddrief M, Julien C (1998) Ionics 4:1
25. Chitra S, Kalyani P, Mohan T, Gangadharan R, Yebka B, Massot M, Julien C, Eddrief M (1999) J Electrochem Soc 3(4):433
26. Guyomard D, Tarascon JM (1991) J Electrochem Soc 138:2864
27. Wan CY, Nuli YN, Wu Q, Yan MM, Jiang ZY (2003) J Appl Electrochem 33:107
28. Miura K, Yamada A, Tanaka M (1996) Electrochim Acta 41:249
29. Ohzuku T, Kitagawa M, Hirai T (1991) J Electrochem Soc 137:769

30. Sphar ME, Novak P, Schnyder B, Haas O, Nesper R (1998) J Electrochem Soc 145:1113
31. Levi MD, Aurbach D (1997) J Phys Chem B 101:4630
32. Levi M D, Levi E A, Aurbach D (1997) J Electroanal Chem 421:89
33. Aurbach D, Levi MD, Levi EA (1998) J Electrochem Soc 145:3024
34. Levi M D, Aurbach D (2004) J Phys Chem B 108:11693
35. Levi M D, Salitra G, Markovsky B, Teller H, Aurbach D (1999) J Electroanal Soc 146:1279